COMETa 2022
6th INTERNATIONAL SCIENTIFIC CONFERENCE
17th - 19th November 2022
Jahorina, B&H, Republic of Srpska
University of East Sarajevo
Faculty of Mechanical Engineering
Conference on Mechanical Engineering Technologies and Applications

EFFICIENCY OF NON-PIN WHEEL CYCLOID REDUCER CONCEPT

Milan Vasić[1], Mirko Blagojević[2], Miloš Matejić[3]

Abstract: Defining new concepts is of vital importance for the further development of cycloid reducers, which are increasingly used in industry. In order to reduce shock loads, backslash, noise, vibrations, and production costs, a new, non-pin wheel concept was developed. However, the use of stationary circular segments instead of rotating ring gear rollers significantly affects the amount of friction. Therefore, this paper aims to analyze the power losses in the contacts of elements of the non-pin wheel cycloid reducer concept. The test was made for different sizes of cycloid reducers, and one of the most acceptable models proposed by Malhotra was used to determine the non-pin wheel concept efficiency. For the calculation of the forces occurring on the basic components, the assumption that it is an ideal meshing case was used. The simulation results show that the greatest power losses occur precisely in the contact between the teeth of the cycloid disc and the stationary circular segments, where sliding friction is dominant.

Key words: cycloid reducers, non-pin wheel concept, efficiency

1 INTRODUCTION

Cycloidal power transmissions are mechanical transmissions that are widely used in robotics, aviation, CNC machines and other branches of industry, and increasingly in electric cars [1,2]. They have compact design, low weight, high transmission ratio, high efficiency, long and reliable work life.

Recent research [3,4] shows that due to the rotation of cycloid discs at high speed, vibrations occur on the rollers of the ring gear due to the impact of the cycloid disc on them (Figure 1). Also, due to the sliding contact between the rollers and the pins of the ring gear, as well as the inability to form an adequate oil film, greater losses occur.

[1] MSc, Milan Vasić, The Academy of Applied Technical Studies Belgrade, The College of Applied Engineering Sciences in Pozarevac, Belgrade, Serbia, mvasic@atssb.edu.rs (CA)
[2] PhD, Mirko Blagojević, University of Kragujevac Faculty of Engineering, Kragujevac, Serbia, mirkob@kg.ac.rs
[3] PhD, Miloš Matejić, University of Kragujevac Faculty of Engineering, Kragujevac, Serbia, mmatejic@kg.ac.rs

Therefore, *Hwang* and *Hsieh* [4] proposed a new cycloid reducer concept where, instead of rotating rollers of the ring gear, stationary circular segments are used that are made flush with the housing, a non-pin wheel concept (Figure 1). In this way, the rolling friction in the contact between the teeth of the cycloid disc and the now stationary circular segments is replaced by the sliding friction. The disadvantage of this concept is that the contact stresses on the sides of the cycloid disc teeth are higher than in the case of the classic concept, and the most significant advantages are: lower shock loads, lower idle speed, lower noise and vibrations [5,6,7]. In the professional literature, there are many papers dealing with the efficiency of cycloid reducers [8,9,10]. *Kudryavtsev* [11] described cycloid reducers in detail and presented a procedure for calculating forces and power losses. In his doctoral dissertation, *Lehmann* [12] built on *Kudryavtsev's* research and modified his method for forces calculation. *Malhotra* [13] derived analytical expressions for calculating the total friction force work on the basis of which the efficiency of the cycloid reducer is determined.

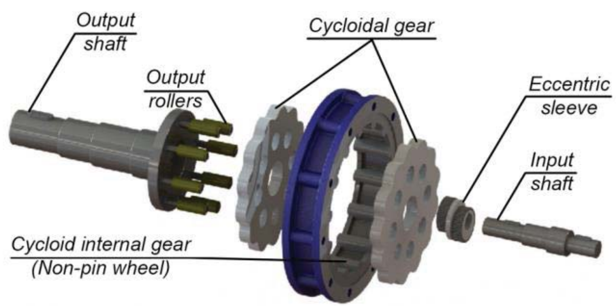

Figure 1. *Disassembled single-stage cycloid reducer of non-pin wheel concept*

Davoli, *Gorla* and others [14] presented the results of the theoretical and experimental analysis of the efficiency of the new cycloid reducer concept. *Pham*, *Bednarczyk* and others [15,16,17] analyzed the dependence of the efficiency on production tolerances as well as inevitable errors during production, which also occur during thermal expansions. *Blagojević* et al. [18] analyzed the dependence of the efficiency on the friction coefficient in the contact between the cycloid disc and the rollers of the ring gear. *Mihailidis* [19] presented a new approach for determining the efficiency, by calculating the friction at each contact point. *Mačkić* [20] investigated the influence of geometrical parameters cycloid reducers efficiency. *Matejić* et al. [21] presented a procedure for determining the efficiency of a two-stage cycloid reducer using *Autodesk INVENTOR* software. *Sensinger* [22] used optimization to increase the efficiency of cycloid reducers. *Olejarczyk* [23] analyzed the impact of installing a sliding and needle bearing on the efficiency, as well as the application of mineral and synthetic oil [24]. Based on the literature review, it can be concluded that researchers are dealing with various aspects to increase efficiency of cycloid reducers. Therefore, the goal of this paper is to determine the value of efficiency of the non-pin wheel concept. The analysis was performed in the MATLAB software package, in which the existing comprehensive expressions for calculating the total friction force work are implemented [13].

2 CYCLOID REDUCER LOADS

During the operation of the cycloid reducer, a torque (T_1) is generated on the cycloid disc as a result of the action of the driving torque (T_{in}), which is shown in Figure

2. The relationship between the torques is as follows [25,26,27]:

$$T_1 - T_2 + T_{in} = 0 \tag{1}$$

where are: T_2 torque on the ring gear (Nm).

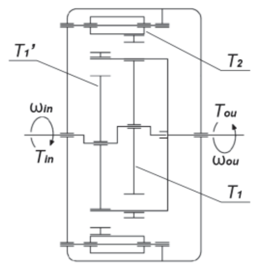

Figure 2. *Kinematic diagram of cycloid reducer, [27]*

In single-stage cycloid reducers where only one cycloid disc is used, if losses are neglected, the torque on the cycloid disc (T_1) is equal to the output torque (T_{ou}), that is, T_1=T_{ou}.

When two cycloid discs are used in a single-stage cycloid reducer, which is the most common case, according to the recommendation from the literature [11,27], the torque on one cycloid disc (T_1) is equal to T_1=0,55·T_{ou}. In this way, the influence of uneven load distribution is taken into account.

The output torque can be determined based on the input torque (T_{in}) and the transmission ratio (u_{CR}):

$$T_{ou} = T_{in} \cdot |u_{CR}| \cdot \eta_{CR} \tag{2}$$

where: η_{CR} – cycloid reducer efficiency.

The torques T_1, T_2 and T_{in} acting on the elements of the cycloid reducer produce three reactions, namely [11-12,25-32]:

- eccentric force - F_E;
- the normal force at the current point of contact between the tooth of the cycloid disc and the roller of the ring gear (normal force) - F_N;
- normal force at the current point of contact between the output rollers and hole in the cycloid disc (output force) - F_K.

The distribution of forces on one cycloid disc is shown in Figure 3 and applies both to the classic and to the non-pin wheel conception of the cycloid reducer. On the second cycloid disc, which is not shown, and is rotated by 180° in relation to the first cycloid disc, exactly the same forces act, and for this reason only one cycloid disc will be considered in the further discussions.

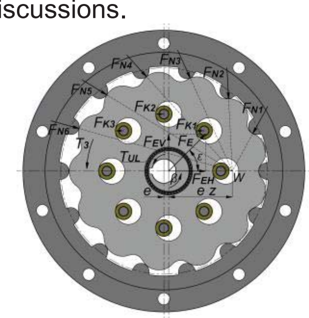

Figure 3. *Distribution of forces and torques acting on cyclid discs in the initial position*

Theoretical models from the literature are used to calculate the normal (F_N) and output force (F_K) [11,12,27]. However, these models do not take into account the modifications of the cycloid disc tooth profile as well as the elastic deformations of the elements participating in the load transfer process [25].

In the theoretical case, when there are no clearances in the cycloid reducer, both cycloid discs are in contact with half of the rollers of the ring gear and the output rollers that participate in the load transfer process. However, in practice this is not the case because there are gaps: due to production, easier assembly and disassembly, better lubrication [33]. The size of the gap directly affects the number of rollers that are in contact with the cycloid disc, so that with an increase in the gap, the number of loaded rollers decreases [34]. Therefore, the calculated force values should be considered approximate.

The normal force on the i-th roller of the ring gear is determined according to expression (3) [12,27]:

$$F_{N\mathrm{i}} = (c \cdot \Delta\beta) \cdot r_1 \cdot \sin\psi_{\mathrm{i}} \tag{3}$$

where: c – stiffness of the roller of the ring gear (N/mm); $\Delta\beta$ – angular rotation of cycloid disc (°); r_i – distance between the point of contact of the i-th roller of the ring gear and cycloid disc measured from the center of the cycloid disc (mm); ψ_i – the angle of direction of the normal force (F_{Ni}) [27].

The output force on the j-th roller is determined according to the equation [12,27]:

$$F_{K\mathrm{i}} = (c_{\mathrm{K}} \cdot \Delta\varphi) \cdot r_{\mathrm{Ki}} \cdot \sin\psi_{\mathrm{Ki}} \tag{4}$$

where: c_K – stiffness of the output roller (N/mm); $\Delta\varphi$ – small angular displacement of cycloid disc (°); r_{Kj} – the distance between the point of contact of the j-th output roller and the cycloid disc measured from the center of the cycloid disc (mm); ψ_{Kj} – the angle between the output force (F_{Kj}) on the j-th output roller and the direction connecting the point of contact of that same roller and cycloid disc with the center of the cycloid disc (°).

The eccentric force is determined as the resultant of the horizontal (F_{EH}) and vertical (F_{EV}) components [12,27,35]:

$$F_{\mathrm{E}} = \sqrt{F_{\mathrm{EH}}^2 + F_{\mathrm{EV}}^2} \tag{5}$$

The horizontal component of the eccentric force is determined based on the equation:

$$F_{\mathrm{EH}} = \sum_{i}{}^{`} F_{\mathrm{Ni}} \cdot \sin x_i + \sum_{j}{}^{`} F_{\mathrm{Kj}} \tag{6}$$

where: x_i – angle between the meshing force of the i-th roller of the ring gear and the vertical direction (°).

The vertical component of the eccentric force is determined according to the equation:

$$F_{\mathrm{EV}} = \frac{T_{\mathrm{in}}}{e} \tag{7}$$

where: e - eccentricity size (mm).

3 NON-PIN WHEEL CYCLOID REDUCER POWER LOSES

The procedure for determining the efficiency of the cycloid reducer is based on the calculation of the total power losses that occur due to overcoming the resistance to the movement of rotating elements in mutual contact.

Table 1. *Presentation of identified contacts that cause resistance to movement*

Contact of a needle bearing with an eccentric cam and a cycloid disc – (a) (rolling friction)
Contact of output rollers with cycloid disc – (b) (rolling friction)
Contact of the stationary circular segments of the ring gear with the cycloid disc - (c) (sliding friction)
Contact between output rollers and pins – (d) (sliding friction)

Identified contacts in cycloid reducers of the non-pin wheel concept that cause movement resistance are shown in Table 1, while their locations are shown in Figure 4. At the same time, the power losses in the sealing elements and bearings were neglected, except for the cycloid disc bearing.

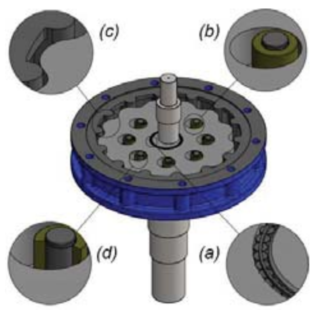

Figure 4. *Locations of contacts that cause resistance to movement in the non-pin wheel design of cycloid reducers*

It should be emphasized that with the non-pin wheel concept, the rolling friction between the rollers of the ring gear and the cycloid disc teeth is replaced by the sliding friction between the stationary circular segments of the ring gear and the cycloid disc teeth. Also, with the non-pin wheel concept, the contacts between the rollers and the pins of the ring gear are lost, thus reducing the corresponding power losses compared to the classic concept.

4 MATHEMATICAL MODEL FOR CALCULATING THE EFFICIENCY OF NON-PIN WHEEL CYCLOID REDUCER CONCEPT

Determining the efficiency of the cycloid reducer [13] is based on the calculation of the total work of the friction force (W_M) and its implementation in the equation:

$$\eta_{CR} = \frac{T_{in} \cdot 2\pi - W_M}{T_{in} \cdot 2\pi} \tag{8}$$

The total work of the friction force represents the integral of the total elementary work dW for a period of one revolution of the input shaft, i.e. $1/z_1$ revolution of the cycloid disc:

$$W_M = \int_0^{\frac{2\pi}{z}} dW \tag{9}$$

where: z_1 – number of cycloid disc teeth.

The total elemental work dW for the non-pin wheel concept includes: elemental work of friction in the cycloid disc bearing (dW_1), elemental work of rolling friction between the output rollers and holes in the cycloid disc (dW_2), elemental work of sliding friction between the cycloid disc and of stationary circular segments of the ring gear (dW_3) and elementary work of sliding friction between output rollers and pins (dW_4).

$$\mathrm{d}W = \mathrm{d}W_1 + \mathrm{d}W_2 + \mathrm{d}W_3 + \mathrm{d}W_4 \tag{10}$$

The elementary work due to friction in the cycloid disc bearing (dW_1) can be determined based on the equation:

$$\mathrm{d}W_1 = f_{\mathrm{r1}} \cdot F_{\mathrm{E}}(\beta) \cdot \frac{D_{\mathrm{SR}}}{d_{\mathrm{kt}}} \cdot z_1 \cdot \mathrm{d}\beta \tag{11}$$

where: $f_{r1}=\mu_{r1} \cdot d_{kt}/2$ – rolling resistance arm of cycloid disc bearing (mm); μ_{r1} – coefficient of rolling friction in cycloid disc bearing; $F_E(\beta)$ - current value of eccentric force (N); $D_{SR}=(D_{CZ}+d_{CZ})/2$ – mean diameter of cycloid disc bearing (mm); D_{CZ} – outer diameter of cycloid disc bearing (mm); d_{CZ} – internal diameter of cycloid disc bearing (mm); d_{kt} – diameter of the rolling body (pin, roller, ball) in the cycloid disc bearing (mm); β – driving angle (°).

The elementary work of the rolling friction between the output rollers and the opening in the cycloid disc (dW_2) can be determined based on the equation:

$$\mathrm{d}W_2 = f_{\mathrm{r2}} \cdot \sum_{j=1}^{q} F_{\mathrm{Kj}}(\beta) \cdot z_1 \cdot \mathrm{d}\beta \tag{12}$$

where: $f_{r2}=\mu_{r2} \cdot D_{VK}/2$ – rolling resistance arm of the output roller (mm); μ_{r2} – coefficient of rolling friction between the output rollers and the opening in the cycloid DISC; D_{VK} – diameter of output roller (mm); $F_{Kj}(\beta)$ - current value of the output force on the j-th output roller (N); q – the current number of output rollers participating in meshing with the cycloid disc. If the total number of output rollers is an even number, then $q=u/2$, and if it is odd, then $q=(u-1)/2$.

The elementary work of the sliding friction between the cycloid disc and the stationary circular segments of the ring gear (dW_3) can be determined based on the equation:

$$\mathrm{d}W_3 = \mu_{\mathrm{s3}} \cdot \sum_{i=1}^{p} F_{\mathrm{Ni}}(\beta) \cdot \frac{D_0}{2} \cdot (z_1 + 1) \cdot \mathrm{d}\beta \tag{13}$$

where: μ_{s3} – the sliding friction coefficient between the fixed circular segments and the cycloid disc, $F_{Ni}(\beta)$ – the current value of the normal force on the i-th segment of the ring gear (N); D_0 – diameter of the circular segment (mm); p – the current number of circular segments participating in the load transfer process. If the total number of circular segments p is an even number, then $p=z_2/2$, and if it is odd, then $p=(z_2+1)/2$.

The elementary work of sliding friction between output rollers and pins (dW_4) can be determined based on the equation:

$$\mathrm{d}W_4 = \mu_{\mathrm{s1}} \cdot \sum_{j=1}^{q} F_{\mathrm{Kj}}(\beta) \cdot \frac{d_{\mathrm{VK}}}{2} \cdot z_1 \cdot \mathrm{d}\beta \tag{14}$$

where: μ_{s1} – sliding friction coefficient between output rollers and pins; d_{VK} – diameter of output rollers (mm). The total work of the friction force W of the non-pin wheel design is calculated based on the comprehensive equation:

$$W = \frac{f_{\mathrm{r1}} \cdot D_{\mathrm{SR}} \cdot z_1}{d_{\mathrm{kt}}} \int_0^{\frac{2\pi}{z_1}} F_{\mathrm{E}}(\beta) \cdot \mathrm{d}\beta + z_1 \cdot \left(f_{\mathrm{r2}} + \frac{\mu_{\mathrm{s1}} \cdot d_{\mathrm{VK}}}{2} \right) \int_0^{\frac{2\pi}{z_1}} \sum_{j=1}^{q} F_{\mathrm{Kj}}(\beta) \cdot \mathrm{d}\beta + (z_1 + 1) \cdot \left(\frac{\mu_{\mathrm{s3}} \cdot D_0}{2} \right) \int_0^{\frac{2\pi}{z_1}} \sum_{i=1}^{p} F_{\mathrm{Ni}}(\beta) \cdot \mathrm{d}\beta \tag{15}$$

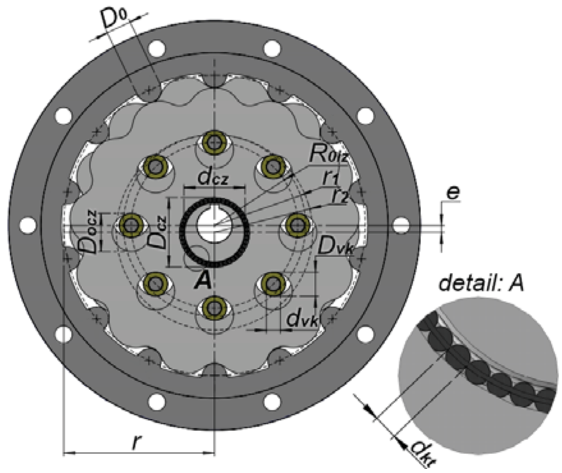

Figure 5. *Dimensions of the cycloid reducer vital elements*

5 EFFICIENCY ANALYSES OF NON-PIN WHEEL CONCEPT

The analysis of the cycloid reducer efficiency of the non-pin wheel concept is based on the testing of cycloid reducers of different sizes.

Therefore, for the purposes of this research, the values of certain parameters [36] were taken from the Sumitomo company catalog, namely input power P_{ul}=(2.2; 3; 4; 5.5; 7.5; 11) kW and transmission ratios u_{CR}=(11; 13; 15; 17; 21; 25). The data for the standard RPM's of the electric motor were taken from the catalog of the company ATB Sever [37] and it is n_{in} =(600; 750; 1000; 1500; 3000) min^{-1}.

The theoretical value of the efficiency largely depends on the adopted values of the friction coefficients of sliding (μ_s) and rolling (μ_r). At the same time, these values are not constant during the reducer operation, and depend on the lubrication regime, working temperatures, the quality of the processed surfaces, the load on the rollers and other factors.

Therefore, the impact of different values of friction coefficients on the efficiency was primarily tested. The test was performed with the assumption that all the individual friction coefficients of sliding (μ_s) and rolling (μ_r) have the same values. Specific sizes of vital elements were used for research: D_{CZ}=40 mm; d_{CZ}=35 mm; d_{kt}=5 mm; z_1=13; z_2=14; D_{VK}=10,4 mm; d_{VK}=5,2 mm; D_0=14 mm; u=8; P_{in}=4 kW.

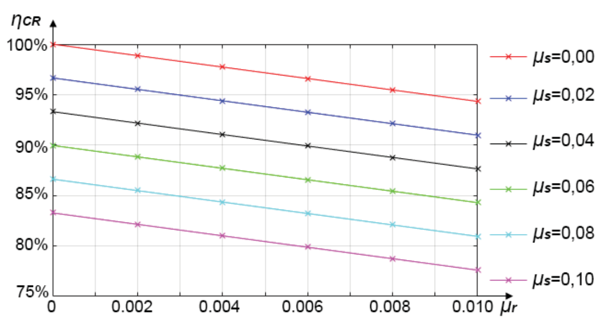

Figure 6. *Dependence of the efficiency on different values of friction coefficients*

Table 2 shows the recommended values of sliding and rolling friction coefficients taken from the literature, while Table 3 shows their adopted values. From Figure 6, it is obvious that with the increase in friction coefficients, the efficiency has a decreasing trend.

Table 2. *Recommended values of sliding and rolling friction coefficients*

	μ_{r1}	μ_{r2}	$\mu_{s1}= \mu_{s2}$	μ_{s3}
[11]			0,07	
[13]			0,01÷0,08	
[38]	0,005			
[39]		0,006		
[40]		0,003	0,03	
[41]				0,03÷0,05

Table 3. *Adopted values of sliding and rolling friction coefficients*

μ_{r1}	μ_{r2}	$\mu_{s1}= \mu_{s2}$	μ_{s3}
0,005	0,0045	0,05	0,004

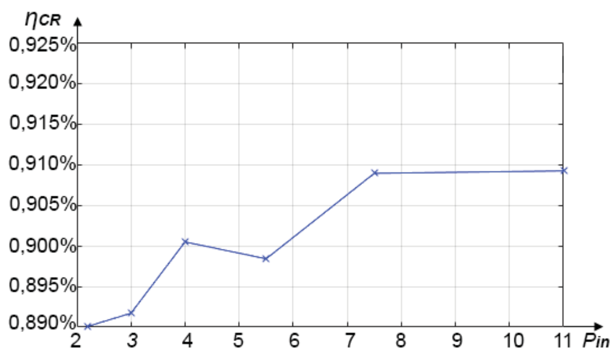

Figure 7. *Dependence of the efficiency on the input power*

The dependence of the efficiency (η_{CR}) on the input power (P_{in}) at a constant transmission ratio u_{CR}=13 and the input speed n_{in}=1500 min^{-1} is shown in Figure 7. The input power varies in an interval of 2,2 kW to 11 kW. With an increase in input power, the efficiency of the cycloid reducer also increases.

The dependence of the efficiency (η_{CR}) on the transmission ratio (u_{CR}) at constant power P_{in}=4 kW and input speed n_{in}=1500 min^{-1} is shown in Figure 8. The transmission ratio varies in the range from 11 to 25. With an increase in the transmission ratio, the efficiency of the cycloid reducer decreases because the number of contacts of the circular segments with the cycloid disc increases.

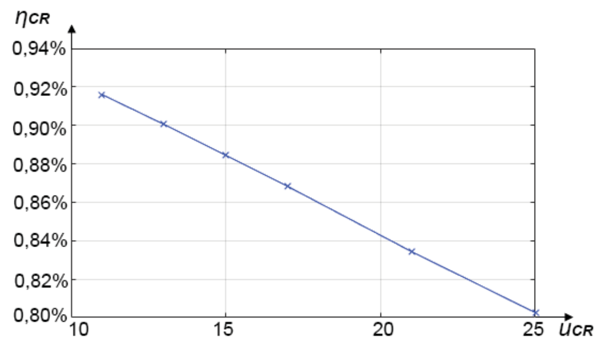

Figure 8. *Dependence of the efficency on the transmission ratio*

Partial losses in the identified contacts have a different distribution in the calculated efficiency, so it is necessary to know their distribution.

The dependence of the partial power losses (W_1,W_2,W_3,W_4) on the input power (P_{in}) at a constant transmission ratio u_{CR}=13 and the input speed n_{in}=1500 min^{-1} are shown in Figure 9.

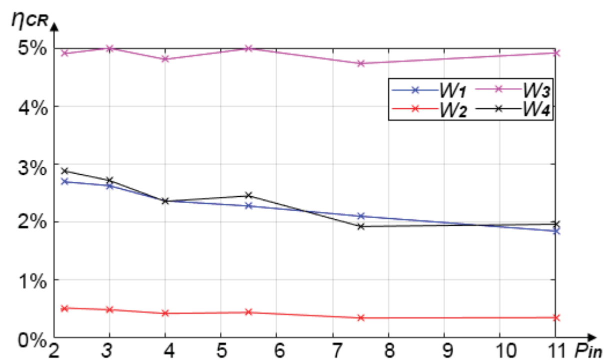

Figure 9. *Dependence of partial power losses on input power*

The biggest power losses occur in the contact of the stationary circular segments with the cycloid disc (W_3=4.73% ÷ 4.99%), which causes a lower efficency of the non-pin wheel concept. Also, significant power losses occur in the contacts of the output rollers and pins (W_4=1.92% ÷ 2.88%), as well as in the cycloid disc bearing (W_1=1.84% ÷ 2.66%). The losses in the contact of the output rollers with the openings in the cycloid disc are significantly lower compared to the previously mentioned ones.

Dependence of partial power losses (W_1,W_2,W_3,W_4) on transmission ratio (u_{CR}) at constant power P_{in}=4 kW and input speed n_{in}=1500 min^{-1} are shown in Figure 10.

The greatest power losses occur in the contact of stationary circular segments with cycloid disc (W_3=4.12% ÷ 8.44%). Also, significant power losses occur in the contacts of the output rollers and pins (W_4=1.83% ÷ 6.14%), as well as in the cycloid disc bearing (W_1=2.12% ÷ 4.06%).

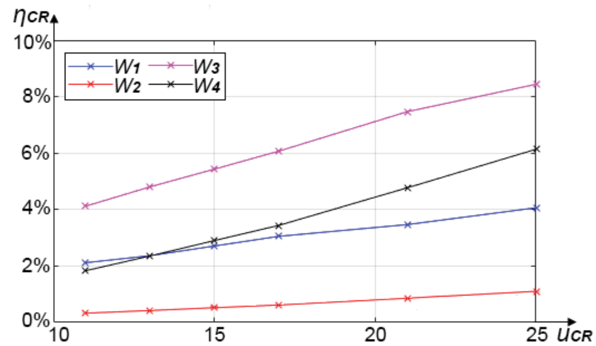

Figure 10. *Dependence of partial power losses on transmission ratio*

6 CONSCLUSION

This paper presents an analysis of the value of the efficiency of the relatively new, non-pin wheel concept of the cycloid reducer. The test was made for different sizes of catalog cycloid reducers.

The detailed analysis provides a good theoretical basis and help for further improvements of the cycloid reducer of the non-pin whel concept, as it indicates the locations of the contacts with the highest power losses.

In the analysis, the Malhotra model was used, which takes into account the losses in the cycloid disc bearing, on the output rollers, pins and on stationary circular segments. The input power of the cycloid reducer, the transmission ratio and the input speed were varied.

Research has shown that with an increase in the transmission ratio, the efficiency of the cycloid reducer decreases because the number of contacts of the circular segments with the cycloid disc increases. Increasing the input power has a positive effect on the efficency.

The largest individual loss occurs in the contact of the stationary circular segments of the ring gear with the cycloid disc (4.12÷8.44%) for the tested cycloid reducer sizes). It is precisely this loss that causes the lower value of the efficiency of the non-pin wheel concept.

In future research, it would be very useful to investigate the possibilities of reducing these losses by using new materials and more efficient types of lubrication.

REFERENCES

[1] Pham A.D., Ahn H.J. (2018). High Precision Reducers for Industrial Robots Driving 4th Industrial Revolution: State of Arts, Analysis, Design, Performance Evaluation and Perpective, International Journal of Precision Engineering and Manufacturing-Green Technology, Vol. 5, No. 4, pp. 519-533.

[2] Li X., Chen B., Wang Y., Sun G., Lim C. T. (2015). Geometry Design of a Non-Pin Cycloid Drive for In-Wheel Motor, SAE Technical Papers 2015.

[3] Chiu-Fan Hsieh (2014). Dynamics Analysis of Cycloidal Speed Reducers With Pinwheel and Nonpinwheel Designs, Journal of Mechanical Design, Volume 136, No. 9, pp. 11.

[4] Hwang Y. W., Hsieh C. F. (2007). Geometric Design Using Hypotrochoid and Nonundercutting Conditions for an Internal Cycloidal Gear, Journal of mechanical design, Vol. 129, No. 4, pp. 369-463.

[5] Wang Y. Liu G., Yu H., Mao H., He K. (2017). Analysis of Meshing Characteristics of Pin sand Pin Housing Integral Structure in Cycloidal Planetary Drive, Conference: ASME 2017 International Mechanical Engineering Congressand Exposition, Vol. 2, pp. 8.
[6] Chen Z., Ou Y., Long S., Peng W., Yang Z. (2018). Vibration Characteristics Analysis of the New Pin-Cycloid Reducer, Journal of the Braziian Society of Mechanical Sciences and Engineering, Vol. 40, pp. 1-17.
[7] Matejić M. (2019). A new approach to the design and optimization of cycloidal power transmissions, PhD thesis, Faculty of Engineering, University of Kragujevac, Kragujevac.
[8] Tonoli A., Amati N., Impinna F., Detoni J., Ruzimov S., Gasparin E., Abdivakhidov K. (2013). Influence of Dry Friction on the Irreversibility of Cycloidal Speed Reducer, World Tribology Congress 2013, September 8-13, 2013, Torino, Italy.
[9] Huang C.H., Tsai S.J. (2017). A Study on Loaded Tooth Contact Analysis of a Cyloid Planetary Gear Reducer Considering Friction and Bearing Roller Stiffness, Journal of Advanced Mechanical Design, Systems, and Manufacturing, Vol. 11, No. 6, pp. 1-17.
[10] Concil F., Maccioni L., Gorla C. (2020). Development of a Computational Fluid Dynamics Simulation Tool for Lubrication Studies on Cycloidal Gear Sets, International Journal of Computational Methods and Experimental Measurements, Vol. 8, No. 3, pp. 220-232.
[11] Kudryavcev V. N. (1966). Planetarnye peredachi, Masinostroenie, Moscow.
[12] Lehmann M. (1976). Calculation and measurement of forces acting on cycloidal speed reducer, Doktorska disertacija, The Technical University of Munich, Munich.
[13] Malhotra S. K., Parameswaran M. A. (1983). Analysis of a cycloid speed reducer, Mechanism and Machine Theory, Vol. 18, No. 6, pp. 491-499.
[14] Davoli P., Gorla C., Rosa F., Longoni C., Chiozzi F., Samarani A. (2007). Theoretical and experimental analysis of a cycloidal speed reducer, International Design Engineering Technical Conferences and Computers and Information in Engineering Conference, , Vol. 7, pp. 1043-1051.
[15] Pham A.D., Ahnb H. J. (2017). Efficiency Analysis of a Cycloid Reducer Considering Tolerance, Journal of Friction and Wear, Vol. 38, pp. 490–496.
[16] Bednarczyk S.,(2019). Determining Power Losses in the Cycloidal Gear Transmission Featuring Manufacturing Deviations, Proceedings of the 14th International Scientific Conference: Computer Aided Engineering, pp. 55-63.
[17] Bednarczyk S. , Jankowski L., Krawczyk J. (2019). The influence of eccentricity changes on power losses in cycloidal gearing, Tribologia, Vol. 3, pp. 19-29.
[18] Blagojevic M., Kocić N., Marjanović M., Stojanović B., Đordevic Z., Ivanović L., and Marjanović N., 2012, “Influence of the Friction on the Cycloidal Speed Reducer Efficiency,” J. Balkan Tribol. Assoc., 18(2), pp. 217–227.
[19] Mihailidis A., Athanasopoulos E., Agouridas K. (2016). EHL film thickness and load dependent power loss of cycloid reducers, Proceedings of the Institution of Mechanical Engineers Part C Journal of Mechanical Engineering Science, Vol. 230, pp. 1303-1317.
[20] Mackić, T., Blagojević M., Babić Z., and Kostić N., (2013). Influence of Design Parameters on Cyclo Drive Efficiency, J. Balkan Tribol. Assoc., 19(4), pp. 167–179.
[21] Matejić M., Blagojević M., Kostić N., Petrović N., Marjanović N. (2019). Analysis of efficiency of a new two stage cycloid drive concept, 16th International Conference on Tribology SERBIATRIB 2019, pp. 335-340.

[22] Sensinger J. (2010). Unified Approach to Cycloid Drive Profile, Stress, and Efficiency Optimization. Journal of Mechanical Design, Vol. 132, No. 2.
[23] Olejarczyk K., Wiklo M., Kolodziejczyk K. (2018). Change of the cycloidal gearbox efficiency for different kind of bearings, sleeves vs. needle bearings, INTERNATIONAL GEAR CONFERENCE 27th-29th August 2018 Lyon Villeurbanne, pp. 87-97.
[24] Olejarczyku K., Wiklo M., Krol K., Kołodziejczyk K. (2017). Obliczenia teoretyczne oraz pomiary stanowiskowe sprawności przekładni cykloidalnej, Modelowanie inżynierskie, Vol. 33, No. 64, pp. 74-81
[25] Chmurawa M., John A., (2000). FEM in Numerical Analysis of Stress and Displacement Distributions in Planetary Wheel of Cycloidal Gear, International Conference on Numerical Analysis and Its Applications, pp. 772-779.
[26] Chmurawa M., Lokiec A. (2001). Distribution of Loads in Cycloidal Planetary Gear (CYCLO) Including Modification of Equidistant, 16th European ADAMS User Conference, Berchtesgaden, Germany.
[27] Blagojević M. (2003). Kinematic and Dynamic Analysis of One-Stage Cycloidal Speed Reducer, Master Thesis, Faculty of Mechanical Engineering, Kragujevac.
[28] Efremenkov E.A., Bonnard E. (2019). Power Parameters Automated Calculation for Transmission with Intermediate Rolling Bodies and Free Cage, MEMT-2019, IOP Conf. Series: Materials Science and Engineering 795.
[29] Tsai S.J., Chang L.C., Huang C.H. (2017). Design of Cycloid Planetary Gear Drives with Tooth Number Difference of Two, Forsch Ingenieurwes, Vol. 81, pp. 325-336.
[30] Wiklo M., Krol R., Olejarczyk K., Kolodziejczyk K. (2019). Output Torque Ripple for a Cycloidal Gear Train, Journal of Mechanical Engineering Science, pp. 1-12.
[31] Xu L.X. (2018). A dynamic Model to Predict the Number of Pins to Transmit Load in a Cycloidal Reducer with Assembling Clearance, Journal of Mechanical Engineering Science, pp. 1-23.
[32] Zhang T., Li X., Wang Y., Sun L. (2020). A Semi-Analytical Load Distribution Model for Cycloid Drives with Tooth Profile and Longitudinal Modifications, Applied Sciences, Vol. 10, pp. 1-19.
[33] Blagojević M., Marjanović N., Djordjević Z., Stojanović B., Marjanović V., Vujanac R., Disić A. (2014). Numerical and experimental analysis of the cycloid disc stress state, Tehnički vjesnik, Vol. 21, No. 2, pp.377-382.
[34] Lixing L., Xin L., Weidong H., Yuanmei Q. (1997). Accurate force analysis in cycloid drive, International Symposium "Machines and Mechanisms", Belgrade, Serbia, pp.1-4.
[35] Jankevich M., Lazurenko Y. (2003). The analysis of loads and selection of efficient geometrical parameters of cicloid gearboxes, International conference Power transmissions.
[36] Sumitomo catalogue
[37] ATB Sever catalogue
[38] SKF Catalogue (2015). Needle roller bearings.
[39] Zhu C., Liu M., Du X., Xiao N., Zhang B. (2010). Analysis on Transmission Characteristics of New Axis-fixed Cycloid Gear, Conference Advanced Materials Research, Vol. 97-101, pp. 60-63
[40] Mačkić T., Babić Ž., Kostić N., Blagojević M. (2013), Cyclo drive efficiency, 13th International Conference on Tribology - Serbiatrib'13, pp. 230-233.
[41] Shipley E. F. (1958). How to Predict Efficiency of Gear Trains, Product Engineering, Vol. 29, No. 31.

View publication stats